Filtration Performance of Dual-layer Filter Paper with Fibrillated Nanofibers

Yunzhen Yao,[a] Min Tang,[a,]* Tian Yu,[b] Yun Liang,[a] and Jian Hu [a]

Filter paper can be dramatically improved by the slip-flow effect and the huge specific surface area of nanofibers. Nanofibers can provide significant improvement in filtration efficiency with a relatively small reduction in permeability. In this study, nanofiber was prepared by fibrillation method using para-aramid fiber. A lab method was developed to laminate the nanofiber layer on a paper substrate by a wet-laid method. The filtration performance of dual-layer filter paper with fibrillated nanofibers was evaluated, and a theoretical model was developed to study the impact of nanofiber diameter on the filtration properties. It is found that in the fibrillation process, the number of trunk fibers decreased and nanofibers increased. With smaller fiber diameter, the pressure drop and filtration efficiency of dual-layer filter paper increased. Based on fibrous structure analysis, the dual-layer filter paper was able to perform well in self-cleaning filtration. The modeling results for pressure drop and filtration efficiency were close to the tested results, which provide a tool to understand the relationship between nanofiber diameter and filtration performance.

Keywords: Filter paper; Filtration properties; Fibrillated nanofiber; Aramid fiber

*Contact information: a: State Key Laboratory of Pulp and Paper Engineering, South China University of Technology, No. 381, Wushan Road, Guangzhou, Guangdong Province, China 510640; b: Guangxi Watyuan Filtration System Co., Ltd, Potang Centralized Industrial Zone, Yuchai Industrial Park, Yulin, Guangxi Province, China 537005; *Corresponding author: tangminde@163.com*

INTRODUCTION

Asian countries, *e.g.,* China, have experienced an unprecedented high level of $PM_{2.5}$ (particles with aerodynamic diameter ≤ 2.5 μm; Pui *et al*. 2014) concentrations during the past several years, resulting in significant concerns over its adverse effects by the general public. Particle contaminants in the air can negatively impact the reliability and availability of important equipment, such as internal combustion engines and gas turbines. Filtration is applied to the inlet to provide protection against the adverse effects of contaminated air. Unfiltered or less-filtered air can result in temporarily or permanently damaged machinery internal parts (Wilcox *et al*. 2010). To face the challenge of higher particle concentration, air filters with higher filtration efficiencies should be used to sustain the equipment's performance.

Air filter paper is widely used in air intake filters for internal combustion engines and gas turbines. Wood pulp fibers, which can provide bulk, strength, and permeability, are the dominant fiber material in filter paper (Hutten 2007). Among the fiber properties, fiber diameter is a key factor affecting the filtration properties of filter paper, as revealed by various filtration theories (*e.g.*, Kuwabara 1959; Brown 1998). Reducing fiber diameter is the dominant way of increasing filtration efficiency (Hutten 2007).

Theoretical predictions and investigations indicate that, when the fiber diameter is less than 1 μm, the filtration efficiency of filter paper can be dramatically improved by the slip-flow effect and the huge specific surface area of ultra-fine fibers (Kosmider and Scott 2002; Ward 2005; Thakur *et al*. 2013; Wang and Otani 2013).

Grafe *et al*. (2001) reported that nanofibers provided significant increases in filtration efficiency with a relatively small reduction in permeability. Wang *et al*. (2008) investigated the performance of filters with a single nanofiber layer on a substrate and showed that nanofiber filters have better filtration performance for particles larger than approximately 100 nm compared with conventional filters. Podgórski *et al.* (2006), Przekop and Grado (2008), Zhang *et al*. (2010), and Leung *et al*. (2010) also studied the filtration performance of filters with nanofibers coated on a substrate.

Many current studies involve placing a nanofiber layer on a coarse substrate *via* an electrospinning process (Yun *et al*. 2007; Bjorge *et al*. 2009). Electrospinning is a technique for extracting fibers from polymer solutions or melts using high-voltage electric charges (Chang and Chang 2016). There are some advanced technologies, *e.g.* bubble electrospinning (Yang *et al*. 2009) and bubbfil spinning technology (Chen *et al*. 2014), for mass-production of nanofibers. In surface filtration, particles from an air stream tend to build up on the surface of filter media (Hubbe *et al*. 2009). Because a nanofiber layer allows surface loading, which can lead to easy removal of the accumulated particles, it is widely used in self-cleaning systems. Because of its superior surface loading effects, after reverse jet pulse cleaning, the filter can return to near-original condition.

In self-cleaning filtration, the filter is cleaned by a jet pulse with pressure ranging from 80 to 100 psig (Wilcox *et al*. 2010), and thus filter paper should be strong enough to sustain the jet pulse. Unlike hydrogen bonds between cellulose fibers in the paper, there is no such force between electrospun nanofibers and substrate fiber, although the electrospinning web is collected on a substrate that will provide strength and stability. Because of the limited mechanical properties, the electrospun web is very easily damaged by subsequent processing and jet pulses. This problem poses a threat to equipment downstream from the filter.

Nanofiber layers can also be laminated by papermaking or a wet-laid process. There are few reports about this method. This study developed a method to laminate a nanofiber layer on a paper substrate in the lab by a wet-laid method. The advantage of the wet-laid method is the robust nanofiber layer. Hydrogen bonds can exist between nanofibers and substrate fibers, and resin reinforcement can easily be applied in the papermaking process. Nanofibers can also be prepared by refining in the papermaking process. Coarse fibers were fibrillated in the refiner to obtain nanofibers. However, fibrillated nanofibers originating from cellulose fibers are very weak.

In this study, para-aramid fibers were used for nanofiber preparation. Para-aramid fibers are high-performance fibers with remarkable mechanical, physical, and chemical properties, such as excellent specific strength, stiffness, and toughness (Salman *et al*. 2015). Para-aramid nanofibers can bond with other nanofibers and substrate fibers by hydrogen bonds (Nimmanpipug *et al*. 2002). In addition, para-aramid nanofibers can be well-dispersed in water for wet-laid forming. In this study, the cellulose paper substrate was laminated with fibrillated para-aramid nanofibers using a dual-layer paper preparation method developed in the lab. The filtration properties of the dual-layer filter paper were studied.

EXPERIMENTAL

Nanofiber Preparation

The nanofibers employed in this study were prepared from para-aramid fibers (diameter: 14 µm, length: 6 mm, Teijin Aramid, Arnhem, Netherlands). To obtain the nanofibers, the para-aramid fibers were continuously treated in a Valley-Niagara refiner (model: ZQS2-15, SUST Machinery, Xianyang, China). The final Schopper-Riegler beating degree of the fibrillated nanofibers was 77 °SR. Because the fibrillated fibers were composed of coarse and fine fibers, fiber classification was necessary to obtain nanofibers with different fiber diameters. The fibrillated nanofibers were fractionalized into five grades by a Bauer-McNett fiber classifier (model: 203C, Andritz Sprout-Bauer Inc., Muncy, USA), based on TAPPI T233cm-95 (1995), as shown in Fig. 1.

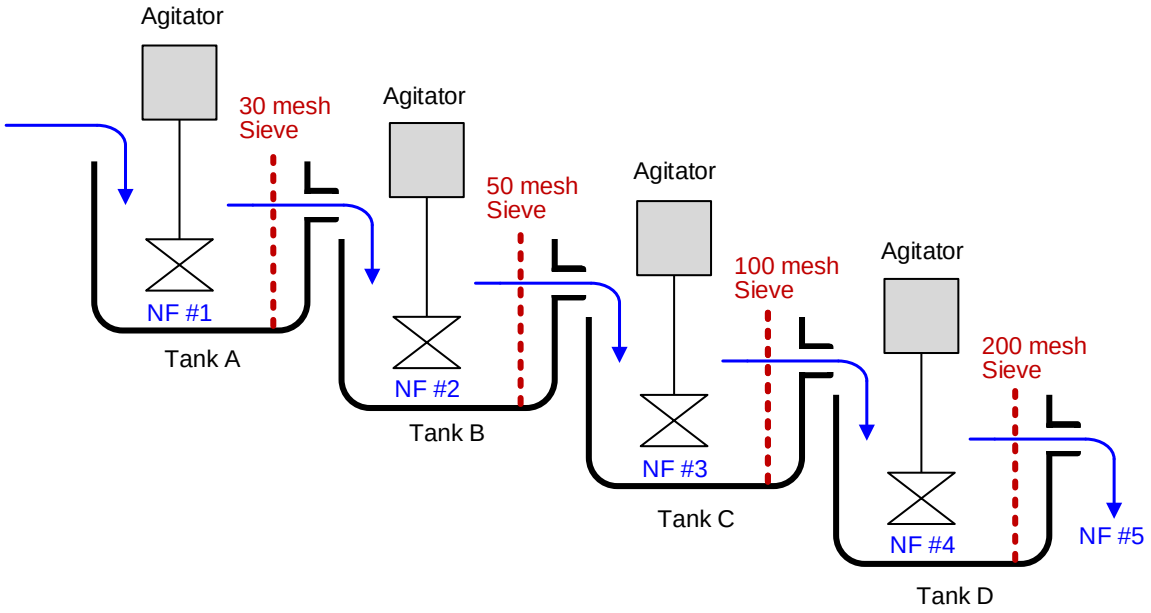

Fig. 1. Schematic diagram of Bauer-McNett fiber classifier

Four different sieves were employed to classify nanofibers, and the opening sizes of sieves are shown in Table 1. The nanofibers obtained from different tanks were collected and labeled NF #1, NF #2, NF #3, and NF #4, respectively. The nanofiber that passed the 200-mesh sieve was labeled NF #5.

Table 1. Nominal Opening Size of Sieves

Sieve Designation	Nominal Sieve Opening Size (mm)
30 mesh	0.595
50 mesh	0.297
100 mesh	0.149
200 mesh	0.074

The key parameter for the nanofibers was fiber diameter. Because the fibrillated nanofibers are very fine, conventional devices, *e.g.*, a Kajaani FS300 fiber analyzer, have difficulty measuring the fiber diameter reliably. In this study, the fiber diameter of each

grade of nanofiber was obtained by measuring 200 fibers manually from scanning electron microscopy (SEM) images.

Dual-Layer Paper Preparation

The dual-layer paper was composed of a paper substrate and nanofiber layer, which were formed by two steps. The first step was the formation of the paper substrate handsheet, which was prepared according to the procedures provided by ISO 5269-1 (2005). The fibers were weighed using an electronic balance with 1 mg accuracy and mixed with 1.5 L of water. The mixture was dispersed in a standard fiber disperser (PTI GmbH, Vorchdorf, Austria) at 3000 rpm for 200 s. The well-dispersed fiber suspension was transferred to a standard handsheet former (PTI GmbH, Vorchdorf, Austria). Then, 5.5 L of water was added to the handsheet former to decrease the fiber consistency and improve the handsheet formation. In addition, 0.08 g of polyamide epichiorobydrin resin (PAE, 12.5% *w.t.*, Guangdong Paper Research Institute, Guangzhou, China) was added to enhance the wet strength of the paper substrate, which was crucial to keep the paper intact during the lamination of the nanofiber layer. After drainage and formation, fibers were retained on the forming wire, forming a wet handsheet. Finally, the wet handsheet was carefully transferred to a dryer and dried at 105 °C for 20 min.

The second step was the lamination of paper substrate and nanofiber layer *via* a wet-laid method, as shown in Fig. 2. The aforementioned nanofiber was more difficult to disperse than cellulose fiber. In this study, a compact blender (model: HR2024, Philips, Zhuhai, China) was used. The compact blender was equipped with serrated blades, which could provide higher shear force than a standard fiber disperser. The weighed nanofibers were mixed with 1.0 L of water and dispersed in the compact blender for 30 min. Inside the standard handsheet former, the dry paper substrate was put on the forming wire in advance. Then, the well-dispersed nanofiber suspension was carefully transferred to the handsheet former without damaging the paper substrate. Because of the addition of PAE, the wet strength of the paper substrate was adequate to keep it from disintegration in water. After drainage and formation, nanofibers were retained on the paper substrate and a nanofiber layer was laminated. The wet dual-layer handsheet was dried at 105 °C for 20 min.

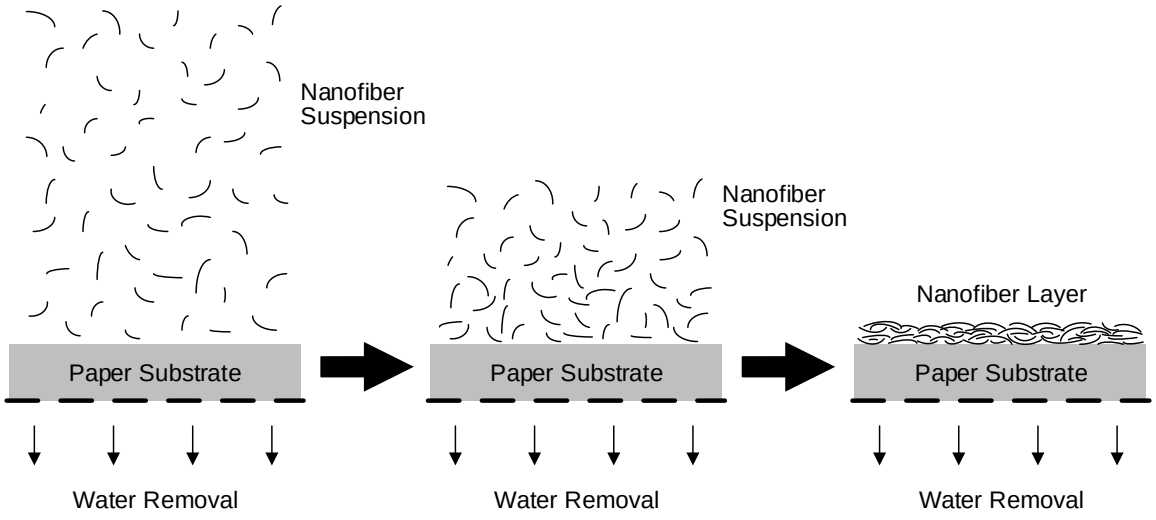

Fig. 2. Nanofiber layer lamination process *via* a wet-laid method

Twelve different kinds of filter paper were prepared. The weight percentage of each fiber in the paper substrate and nanofiber layer can be seen in Table 2. The paper substrate was composed of hardwood fibers and PET fibers. Hardwood fibers (from Suzano Pulp and Paper Inc., São Paulo, Brazil) were flash-dried when manufactured. The unbeaten hardwood fiber was used for paper preparation. The dimensions of the PET fibers (from Kuraray Co., Ltd, Tokyo, Japan) were 0.3 D × 5 mm. Two different kinds of paper substrate were used, and the basic weight was 45 ± 2 g/m^2. The nanofiber layer was purely composed of classified nanofibers, and the basis weight was 2 ± 0.2 g/m^2. The preparation and testing for each type of paper were repeated five times.

Table 2. Weight Percentage of Fibers in Paper Substrate and Nanofiber Layer

No.	Paper Substrate		Nanofiber Layer					Note
	Hardwood	PET	NF #1	NF #2	NF #3	NF #4	NF #5	
1#	80%	20%	-	-	-	-	-	No nanofiber layer
2#	80%	20%	100%	-	-	-	-	Dual-layer
3#	80%	20%	-	100%	-	-	-	Dual-layer
4#	80%	20%	-	-	100%	-	-	Dual-layer
5#	80%	20%	-	-	-	100%	-	Dual-layer
6#	80%	20%	-	-	-	-	100%	Dual-layer
7#	60%	40%	-	-	-	-	-	No nanofiber layer
8#	60%	40%	100%	-	-	-	-	Dual-layer
9#	60%	40%	-	100%	-	-	-	Dual-layer
10#	60%	40%	-	-	100%	-	-	Dual-layer
11#	60%	40%	-	-	-	100%	-	Dual-layer
12#	60%	40%	-	-	-	-	100%	Dual-layer

Filtration Properties Test

The filtration efficiency and pressure drop were measured with a filtration test system based on EN 779 (2012) and ASHRAE 52.2 (2012), as shown in Fig. 3.

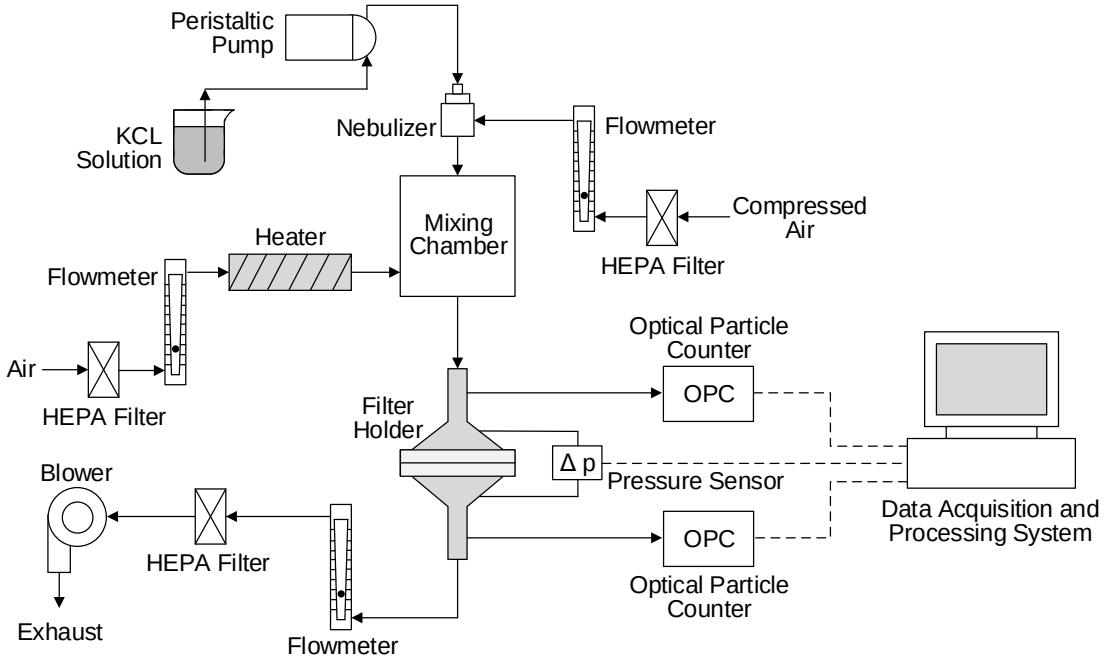

Fig. 3. Schematic diagram of filtration test setup

Unlike EN 779 (2012), in which liquid particles are used to test the efficiency, this study employed a potassium chloride (KCl) aqueous solution with 12% *w.t.* to generate solid particles for testing. As mentioned in ASHRAE 52.2 (2012), solid particles can bounce off the collection fiber surface and usually present a more severe challenge than liquid particles to filter paper used for the filtering of air. In addition, KCl particles are commonly available and benign to human health.

The filter paper was mounted in the filter holder with a test area of 100 cm^2. The upstream and downstream of the filter holder were connected to a pressure sensor and two optical particle counters. The pressure sensor (Model: 166, Range: 0 to 500 Pa, Alpha Instruments Inc., Acton, USA) measured the pressure drop across the filter paper under a set testing velocity. Optical particle counters (Model: SX-L310, Suzhou Sothis, China) were calibrated by NIST traceable polystyrene latex (PSL) particles. The optical particle counter sampled 28.3 L of air per minute constantly from the flow and measured the number concentration of the sampling air for 0.3 to 10 µm particles. The upstream number concentration, $N_{up,i}$, and downstream concentration, $N_{down,i}$, were used to calculate the filtration efficiency, E_i, for particles with a diameter of d_i. The calculation method is shown in Eq. (1). In EN 779 (2012), one of the criteria for filter rating is based on the filtration efficiency of 0.4-µm particles. Therefore, 0.4 µm efficiency was used in this study. In addition, filtration efficiency for 0.8 and 2 µm particles, which were in the regime of $PM_{2.5}$, were employed to evaluate the filtration performance of filter paper laminated with nanofibers.

$$E_i = 1 - \frac{N_{down,i}}{N_{up,i}} \quad (1)$$

A flowmeter (Model: FFM64-15FA, Floworld Limited, Houston, USA) and a downstream ball valve were used to control the flow rate across the filter paper. The flow rate in this study was 60 L/min. Accordingly, the face velocity was 10.0 cm/s, a value that is frequently used in this type of air filter paper. The temperature of the ambient air was between 20 and 28 °C, with a relative humidity of less than 75%.

A theoretical model was deduced from experimental data of filtration test. Since filtration properties are directly determined by the fiber size (Li *et al*. 2015), a simple mathematical relationship between filtration properties and pore size was established. The least squares method in the modeling was conducted in the Solver of Microsoft Excel 2016 using GRG nonlinear solving method.

RESULTS AND DISCUSSION

Nanofiber Characterization

The morphology of nanofibers NF #1, NF #2, NF #3, NF #4, and NF #5 can be seen in the SEM images shown in Fig. 4. In the beating process, the nanofibers were gradually fibrillated from the trunk fibers. From NF #1 to NF #5, the number of trunk fibers decreased and nanofibers increased, until NF #5 obtained the finest morphology. Nanofibers NF #1, NF #2, and NF #3 were not only composed of fine nanofibers, but also a certain amount of partially fibrillated coarse trunk fibers. Those trunk fibers could enhance filtration properties as well as fine nanofibers. There was a remarkable change from NF #3 to NF #4. While NF #3 contained trunk fibers, NF #4 was composed almost entirely of nanofibers. NF #5 was also mostly composed of nanofibers.

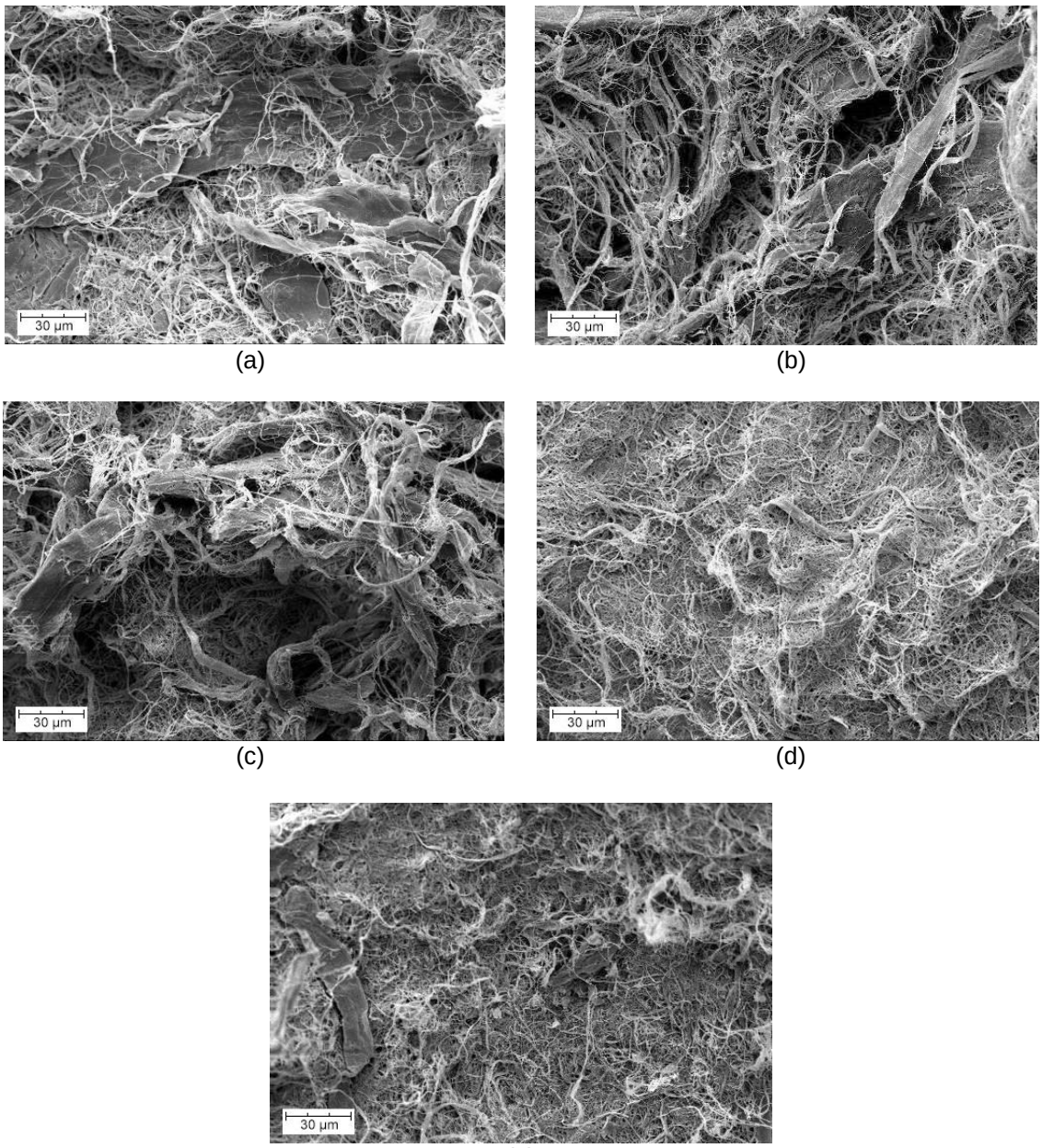

Fig. 4. SEM images of nanofiber; (a) NF #1, (b) NF #2, (c) NF #3, (d) NF #4, and (e) NF #5

The average nanofiber diameter and standard deviation are shown in Table 3. The average diameters of NF #1, NF #2, and NF #3 were much larger than those of NF #4 and NF #5.

As shown in the SEM images, NF #1, NF #2, and NF #3 contained a certain amount of trunk fibers. The 100-mesh sieve could block most of the trunk fibers, and the nanofibers after passing the 100-mesh sieve, namely NF #4 and NF #5, were much finer. The average fiber diameter in Table 3 was used in the following theoretical model for the filtration properties.

Table 3. Average Diameter and Standard Deviation of Nanofiber

Nanofiber	Average Diameter (μm)	Standard Deviation (μm)
NF #1	2.45	1.29
NF #2	1.48	1.15
NF #3	0.91	0.75
NF #4	0.29	0.16
NF #5	0.24	0.11

Filtration Properties of Dual-Layer Filter Paper

The testing results for pressure drop and filtration efficiency are shown in Table 4. For filter paper laminated with a nanofiber layer, both the pressure drop and filtration efficiency increased markedly compared with the paper substrate. Because the fiber diameter decreased from NF #1 to NF #5, the pressure drop and filtration efficiency increased. These results are in good agreement with the observation of SEM images and measurement of fiber diameters for fibrillated nanofibers.

For dual-layer filter paper containing NF #4 and NF #5, the filtration efficiency was about five times that of the paper substrate, which was a large improvement. The filtration efficiencies of NF #4 and NF #5 laminated papers were very similar, but NF #4 laminated paper showed a lower pressure drop, making NF #4 a better choice in terms of filtration performance. It was also found that the substrate had minor effect on the filtration efficiency of the laminated paper.

Table 4. Filtration Properties of Dual-Layer Paper

Sample	Pressure Drop (Pa)	Filtration Efficiency			Note
		0.4 μm	0.8 μm	2 μm	
#1	25.5	0.202	0.241	0.416	No nanofiber layer
#2	57.4	0.379	0.556	0.775	NF #1
#3	62.0	0.492	0.672	0.879	NF #2
#4	72.5	0.532	0.687	0.89	NF #3
#5	381.9	0.942	0.986	0.995	NF #4
#6	458.9	0.948	0.989	0.996	NF #5
#7	16.3	0.165	0.18	0.307	No nanofiber layer
#8	31.3	0.338	0.495	0.706	NF #1
#9	44.4	0.458	0.639	0.835	NF #2
#10	56.7	0.502	0.693	0.875	NF #3
#11	293.7	0.91	0.961	0.983	NF #4
#12	332.9	0.941	0.977	0.991	NF #5

The SEM images of dual-layer filter paper containing nanofibers are shown in Fig. 5. The paper containing NF #4 and NF #5 showed a much smoother nanofiber layer than the others. During operation, if particle contaminants were captured on the nanofiber layer, then the particles could deeply penetrate the open fibrous structure for filter papers containing NF #1, NF #2, and NF #3. However, for filter papers containing NF #4 and NF #5, the particles were mostly captured on the surface of the filter paper. Because the filtration efficiency of NF #4 and NF #5 nanofiber layers were very high, particles could not easily enter the bulk of the filter paper.

In applications like self-cleaning filtration, a reverse jet pulse is periodically applied on the filter to clean the filter. Because the hydrogen bond structure is one of the most characteristic of aramide polymers like para-aramid (Nimmanpipug *et al.* 2002), hydrogen

bonds existed among the para-aramid nanofibers and cellulose fibers of the paper substrate. The interlayer bonding strength between paper substrate and the nanofiber layer was strong enough to sustain the powerful jet pulse and keep the nanofiber layer from being damaged. With high efficiency and smooth surface, the particle cake that accumulated on the nanofiber layer could be easily removed, and fewer particles were retained compared with the open fibrous structure. Thus, filter paper was cleaned and filtration performance was recovered. The structure of paper containing NF #4 and NF #5 enabled it to perform well in self-cleaning filtration. The test system for self-cleaning filtration should be developed for further analysis in the future.

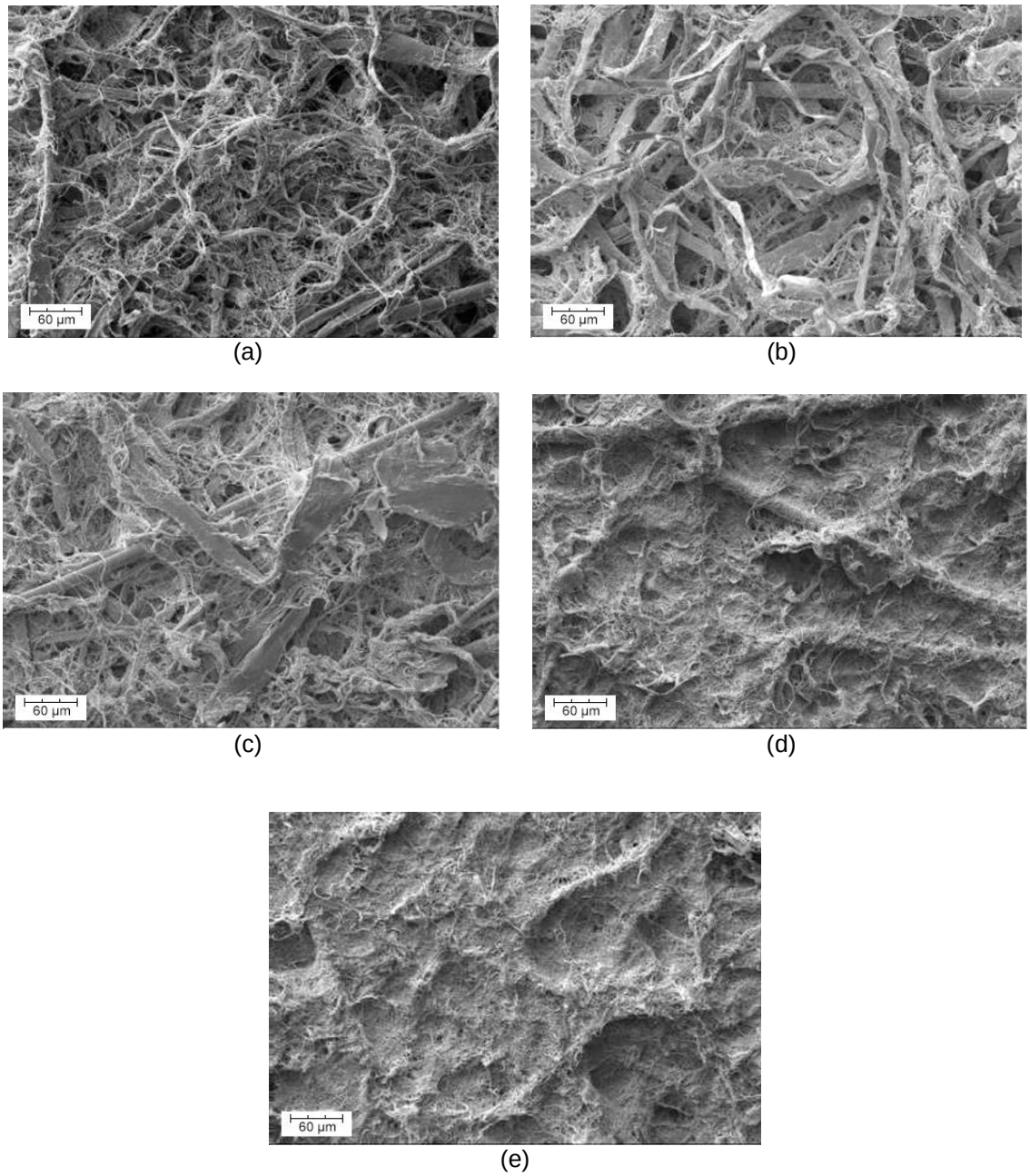

Fig. 5. SEM images of dual-layer filter paper. (a) paper #2, (b) paper #3, (c) paper #4, (d) paper #5, and (e) paper #6

Modeling of Filtration Properties of Dual-Layer Filter Paper

To further study the impact of nanofiber diameter on the filtration properties of dual-layer filter paper, a theoretical model was deduced from experimental data. It is important to notice that the basis weight of the nanofiber layer was not considered in this study.

Assume the pressure drop and filtration efficiency for a particle with a diameter d_i for a paper substrate are Δp_s and $E_{s,i}$, and the enhancement factor for the pressure drop and efficiency resulting from nanofiber lamination are λ_p and λ_E, as defined by Eqs. 2 and 3, respectively. The pressure drop for dual-layer filter paper, Δp, was calculated using Eq. 2. The filtration efficiency for a particle with a diameter d_i for dual-layer filter paper, E_i, was calculated using Eq. 3,

$$\lambda_p = \frac{\Delta p}{\Delta p_s} \tag{2}$$

$$\lambda_E = \frac{\ln\left(1 - E_i\right)}{\ln\left(1 - E_{s,i}\right)} \tag{3}$$

The relationships among λ_p, λ_E, and nanofiber diameter (d_{NF}) can be expressed as Eqs. 4 and 5, respectively, based on trials of various mathematical functions,

$$\lambda_p = a_1 (d_{NF})^{a_2} \tag{4}$$

$$\lambda_E = b_1 (d_{NF})^{b_2} \tag{5}$$

where, a_1, a_2, b_1, and b_2 are constants.

The experimental data were used to calculate the constants in Eqs. 4 and 5 by the least squares method. The values of a_1, a_2, b_1, and b_2 were determined to be 3.651, 1.145, 4.901, and 0.666, respectively.

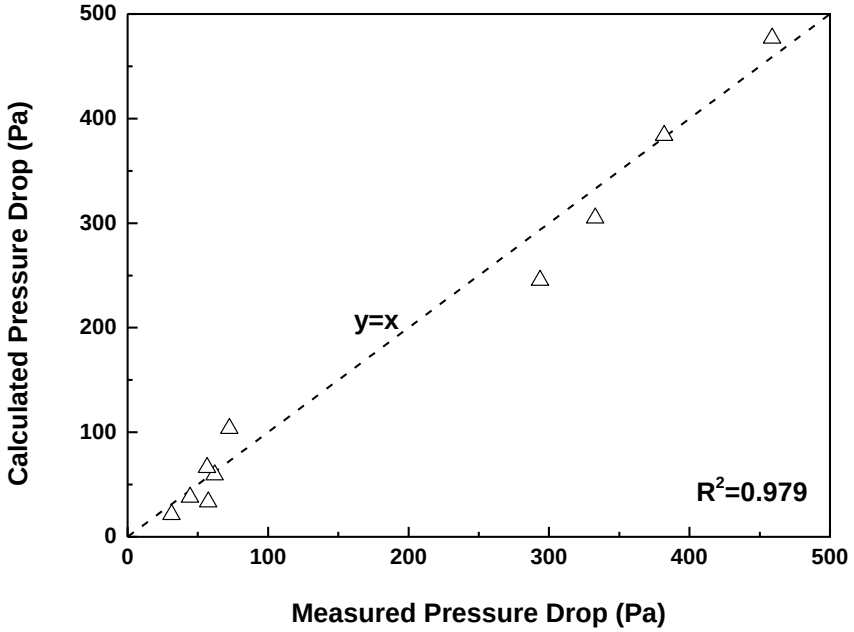

Fig. 6. Modeling and tested values of pressure drop

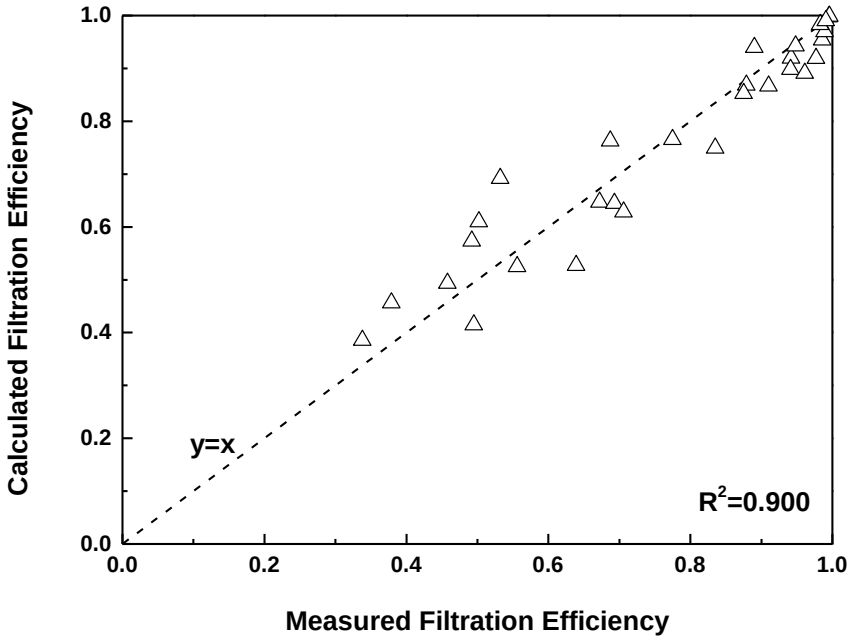

Fig. 7. Modeling and testing values of filtration efficiency

Therefore, the pressure drop and filtration efficiency of the dual-layer filter paper can be calculated using Eqs. 6 and 7, if the filtration properties of the paper substrate and the nanofiber diameter are known,

$$\Delta p = 3.651 \times \Delta p_s (d_{NF})^{1.145} \quad (6)$$

$$E_i = 1 - \exp\left[4.901 \left(d_{NF} \right)^{0.666} \ln\left(1 - E_{s,i}\right) \right] \quad (7)$$

A comparison of the experimental and theoretical data is shown in Figs. 6 and 7. The coefficients of determination were close to 1, which means that the theoretical modeling methods, *via* Eqs. 6 and 7, are reliable. Eqs. 6 and 7 provide a mathematical tool to understand the relationship between nanofiber diameter and filtration performance.

CONCLUSIONS

1. Fibrillated para-aramid nanofibers were obtained using a refiner and fractionalized into five grades. A method was developed to laminate the nanofiber layer on a paper substrate by a wet-laid method.
2. From NF #1 to NF #5, the number of trunk fibers decreased and nanofibers increased, until NF #5 obtained the finest morphology. With decreasing fiber diameter from NF #1 to NF #5, the pressure drop and filtration efficiency of dual-layer filter paper increased. For dual-layer filter paper containing NF #4 and NF #5, the filtration efficiency was approximately five times that of the paper substrate. The structure of dual-layer filter paper containing NF #4 and NF #5 enabled it to perform well in self-cleaning filtration.

3. A theoretical model was developed to study the impact of nanofiber diameter on the filtration properties of dual-layer filter paper. The modeling results for pressure drop and filtration efficiency were close to the tested results, with R^2 values of 0.979 and 0.900, respectively.

ACKNOWLEDGMENTS

The authors are grateful for the support of Guangdong - Hong Kong Generic Technology Bidding Project, Grant. No. 2013B010135003, and Guangzhou Science and Technology Plan Project, Grant. No. 201504010019.

REFERENCES CITED

ASHRAE 52.2 (2012). "Method of testing general ventilation air-cleaning devices for removal efficiency by particle size," *American Society of Heating, Refrigerating and Air-Conditioning Engineers*, Atlanta, GA.

Bjorge, D., Daels, N., De Vrieze, S., Dejans, P., Van Camp, T., Audenaert, W., Hogie, J., Westbroek, P., Clerck, K. D., Stijn, W. H., *et al.* (2009). "Performance assessment of electrospun nanofibers for filter applications," *Desalination* 249(3), 942-948. DOI: 10.1016/j.desal.2009.06.064

Brown, R. C. (1998). "Airflow through filters-beyond single-fiber theory," in: *Advances in Aerosol Gas Filtration*, B. K. Spurny (ed.), 153-172, CRC Press, Boca Raton, Florida.

Chang, C. Y., and Chang, F. C. (2016). "Development of electrospun lignin-based fibrous materials for filtration applications," *BioResources* 11(1), 2202-2213. DOI: 10.15376/biores.11.1.2202-2213

Chen, R., Ya, L., and He, J. (2014). "Bubbfil spinning for mass-production of nanofibers," *Thermal Science* 18(5), 1718-1719. DOI: 10.2298/TSCI1405718C

EN 779 (2012). "Particulate air filters for general ventilation — Determination of the filtration performance," *European Committee for Standardization*, Brussels, Belgium.

Grafe, T., Gogins, M., Barris, M., Schaefer, J., and Canepa, R. (2001) "Nanofibers in filtration applications in transportation," in: *Filtration 2001 International Conference and Exposition of the INDA*, Chicago, Illinois, December 3-5, 2001.

Hubbe, M. A., Chen, H., and Heitmann, J. A. (2009). "Permeability reduction phenomena in packed beds, fiber mats, and wet webs of paper exposed to flow of liquids and suspensions: A review," *BioResources* 4(1), 405-451. DOI: 10.15376/biores.4.1.405-451

Hutten, I. M. (2007). *Handbook of Nonwoven Filter Media*, Butterworth-Heinemann, Oxford, UK. DOI: 10.1016/B978-1-85617-441-1.50004-4

ISO 5269-1 (2005). "Pulps - Preparation of laboratory sheets for physical testing - Conventional sheet-former method," *International Organization for Standardization*, Geneva, Switzerland.

Kosmider, K., and Scott, J. (2002). "Polymeric nanofibres exhibit an enhanced air filtration performance," *Filtration & Separation* 39(6), 20-22. DOI: 10.1016/S0015-1882(02)80187-2

Kuwabara, S. (1959). "The forces experienced by randomly distributed parallel circular cylinders or spheres in a viscous flow at small Reynolds numbers," *Journal of the Physical Society of Japan* 14(4), 527-532. DOI: 10.1143/JPSJ.14.527

Leung, W. W. F., Hung, C. H., and Yuen, P. T. (2010). "Effect of face velocity, nanofiber packing density and thickness on filtration performance of filters with nanofibers coated on a substrate," *Separation and Purification Technology* 71(1), 30-37. DOI: 10.1016/j.seppur.2009.10.017

Li, X. W., Kong, H. Y., and He, J. H. (2015). "Study on highly filtration efficiency of electrospun polyvinyl alcohol micro-porous webs," *Indian Journal of Physics* 89(2), 175-179. DOI: 10.1007/s12648-014-0542-2

Nimmanpipug, P., Tashiro, K., Maeda, Y., and Rangsiman, O. (2002). "Factors governing the three-dimensional hydrogen bond network structure of poly (m-phenylene isophthalamide) and a series of its model compounds:(1) Systematic classification of structures analyzed by the X-ray diffraction method," *The Journal of Physical Chemistry B* 106(27), 6842-6848. DOI: 10.1021/jp013982i

Podgórski, A., Bałazy, A., and Gradoń, L. (2006). "Application of nanofibers to improve the filtration efficiency of the most penetrating aerosol particles in fibrous filters," *Chemical Engineering Science* 61(20), 6804-6815. DOI: 10.1016/j.ces.2006.07.022

Przekop, R., and Gradoń, L. (2008). "Deposition and filtration of nanoparticles in the composites of nano-and microsized fibers," *Aerosol Science and Technology* 42(6), 483-493. DOI: 10.1080/02786820802187077

Pui, D. Y. H., Chen, S. C., and Zuo, Z. (2014). "$PM_{2.5}$, in China: Measurements, sources, visibility and health effects, and mitigation," *Particuology* 13(2), 1-26. DOI: 10.1016/j.partic.2013.11.001

Salman, S. D., Leman, Z., Sultan, M. T., Ishak, M. R., and Cardona, F. (2015). "Kenaf/synthetic and Kevlar®/cellulosic fiber-reinforced hybrid composites: A review," *BioResources* 10(4), 8580-8603. DOI: 10.15376/biores.10.4.salman

TAPPI T233 cm-95 (1995). "Fiber length of pulp by classification," Technical Association of the Pulp and Paper Industry, Peachtree Corners, GA.

Thakur, R., Das, D., and Das, A. (2013). "Electret air filters," *Separation & Purification Reviews* 42(2), 87-129. DOI: 10.1080/15422119.2012.681094

Wang, C. S., and Otani, Y. (2013). "Removal of nanoparticles from gas streams by fibrous filters: A review," *Industrial & Engineering Chemistry Research* 52(1), 5-17. DOI: 10.1021/ie300574m

Wang, J., Kim, S. C., and Pui, D. Y. H. (2008). "Investigation of the figure of merit for filters with a single nanofiber layer on a substrate," *Journal of Aerosol Science* 39(4), 323-334. DOI: 10.1016/j.jaerosci.2007.12.003

Ward, G. (2005). "Nanofibres: Media at the nanoscale," *Filtration & Separation* 42(7), 22-24. DOI: 10.1016/S0015-1882(05)70618-2

Wilcox, M., Baldwin, B., Garcia-Hernandez, A., and Brun, K. (2010). *Guideline for Gas Turbine Inlet Air Filtration Systems*, Southwest Research Institute, San Antonio, TX.

Yang, R., He, J., Xu, L., and Yu, J. (2009). "Bubble-electrospinning for fabricating nanofibers," *Polymer* 50(24), 5846-5850. DOI: 10.1016/j.polymer.2009.10.021

Yun, K. M., Hogan, C. J., Matsubayashi, Y., Kawabe, M., Iskandar, F., and Okuyama, K. (2007). "Nanoparticle filtration by electrospun polymer fibers," *Chemical Engineering Science* 62(17), 4751-4759. DOI: 10.1016/j.ces.2007.06.007

Zhang, Q., Welch, J., Park, H., Wu, C. Y., Sigmund, W., and Marijnissen, J. C. (2010). "Improvement in nanofiber filtration by multiple thin layers of nanofiber mats," *Journal of Aerosol Science* 41(2), 230-236. DOI: 10.1016/j.jaerosci.2009.10.001

Article submitted: May 9, 2016; Peer review completed: July 11, 2016; Revised version received and accepted: September 13, 2016; Published: September 22, 2016.
DOI: 10.15376/biores.11.4.9506-9519